Microelectronic Engineering 277 (2023) 112016

Contents lists available at ScienceDirect

Microelectronic Engineering

journal homepage: www.elsevier.com/locate/mee

Beyond mobile phone displays: Flat panel display technology for biomedical applications

Alfredo Mameli [a], Hylke B. Akkerman [a], Sandra González-Lana [b,c], Héctor Castro-Abril [c], Kim Le Cann [d], Angelika Lampert [d], Gerwin H. Gelinck [a], Auke Jisk Kronemeijer [a], Albert J.J.M. van Breemen [a,*]

[a] TNO/Holst Centre, High Tech Campus 31, 5656 AE Eindhoven, the Netherlands
[b] Instituto de Nanociencia y Materiales de Aragón (INMA), CSIC-Universidad de Zaragoza, Advanced Manufacturing Laboratory, Departamento de Física de la Materia Condensada, C./Pedro Cerbuna 12, 50009 Zaragoza, Spain
[c] BEONCHIP S.L., CEMINEM, Campus Rio Ebro. C./Mariano Esquillor Gómez s/n, 50018 Zaragoza, Spain
[d] Uniklinik RWTH Aachen University, Institute of Physiology (Neurophysiology), Pauwelsstr. 30, 52074 Aachen, Germany

ARTICLE INFO

Keywords:
Flat panel display technology
Microfluidics
Organ-on-chip
Large-area scalable manufacturing

ABSTRACT

Organ-on-Chips (OoCs) have emerged as a human-specific experimental platform for preclinical research and therapeutics testing that will reduce the cost of pre-clinical drug development, provide better physiological relevance and replace animal testing. Yet, the lack of standardization and cost-effective fabrication technologies can hamper wide-spread adoption of OoCs. In this work we validate the use of flat panel display (FPD) technology as an enabling and cost-effective technology platform for biomedical applications by demonstrating facile integration of key OoC modules like microfluidics and micro electrode arrays (MEAs) in the standardized 96-well plate format. Individual and integrated modules were tested for their biological applicability in OoCs. For microelectrode arrays we demonstrate 90–95% confluency, 3 days after cell seeding and >70% of the initial mitochondrial cell activity for microfluidic devices. Thus highlighting the biocompatibility of these modules fabricated using FPD technology. Furthermore, we provide two examples of monolithically integrated microfluidics and microelectronics, *i.e.* integrated electronic valves and integrated MEAs, that showcase the strength of FPD technology applied to biomedical device fabrication. Finally, the merits and opportunities provided by FPD technology are discussed through examples of advanced structures and functionalities that are unique to this enabling platform.

1. Introduction

The aim of organ-on-chips (OoCs) is to build an effective micro-physiological model to characterize (multi-)organ responses to external stimuli, and thus accelerate the understanding of diseases and drug interactions [1–3]. Accelerating the development of personalized pharmaceuticals can be achieved using an engineered *in vitro* model of a specific organ or network thereof that is integrated with a multitude of actuators and sensors. These actuators and sensors would then be capable of driving and monitoring complex parallelized biological experiments with high-throughput [1,4]. In this way, the heavily-used and standardized multi-well plates for pre-clinical studies would become a smart multi-well plate (SMWP) by enriching them with model-systems and functionalities that enable fully-automated biological experiments.

Several SMWP concepts have recently been presented [5], in most of the cases they either have microfluidic or electronic/sensing functionalities, while integration of both functionalities has revealed itself to be rather challenging. In addition, OoC platform standardization and reliable industrial scale production are still lacking. Topics that, as also acknowledged within the European OoC roadmap [6,7], need to be addressed early-on in the development phase to facilitate and speed up worldwide commercial adoption of OoC technology.

The current mainstream approach towards SMWPs focuses mainly on two key modules and the underlying fabrication technology. Microfluidics are largely based on poly(dimethylsiloxane) (PDMS) which has limited scalability and has been reported to be leading to misinterpretation about drug toxicity and efficacy [8]. Thermoplastics like poly (methyl methacrylate) (PMMA) and cyclo olefins (COP, COC) are

* Corresponding author.
E-mail address: albert.vanbreemen@tno.nl (A.J.J.M. van Breemen).

https://doi.org/10.1016/j.mee.2023.112016
Received 16 October 2022; Received in revised form 17 March 2023; Accepted 4 May 2023
Available online 5 May 2023

typically processed by injection moulding, a scalable and high volume technology [9]. Microelectronics are a second key module of SMWPs, which relies on printed circuit board and silicon-based technologies [1,10]. Although these module approaches have led to major advancements, the aspect of microfluidic and microelectronics integration within industry-compatible manufacturing platforms is often overlooked and may in the long run hinder wide-spread adoption from pharmaceutical end-users. For solving the difficulties related to integration of microelectronics and microfluidics, herein we propose the adoption of FPD technology which allows for monolithic integration of both features and, in future, can enable the integration of even more complex functionalities such as pH- and O_2-sensing and optical detection.

FPD embraces deposition, patterning and etching technologies that are scalable to very large substrate sizes, up to GEN10.5 size, *i.e.* 284 × 337 cm^2, thereby enabling cost-effective production and commercialization of displays [11]. Smith et al. have already highlighted how wearable biomedical devices can benefit from low-cost FPD manufacturing (<10 cents/cm^2 with production rates larger than 100 km^2/year) [12] and some work in this respect has been undertaken by our group as well [13]. In this work, we stretch the applicability of FPD technology to realize microfluidics with integrated microelectronics, like micro electrode arrays, and highlight it as a cost-effective and viable mass-manufacturing platform technology for biological devices, such as lab-on-chip and organ-on-chip. Although FPD is a well-established high-volume manufacturing technology, very little is known about the compatibility of FPD materials and processing with biological matter. Since biocompatibility is an essential requirement for *e.g.* cell-culturing [2], we fabricated microfluidic and microelectronic modules for OoC applications and tested the biocompatibility thereof. Furthermore, we highlight the advantages of FPD technology that might fast-forward the adoption of OoC devices, with particular focus on SMWP.

2. Experimental

2.1. Micro electrode array fabrication and integration

First a polyimide-precursor (DuPont) is deposited on a glass carrier (1.1 mm, EAGLE XG®, Corning Inc.) and cured, resulting in a polyimide foil with a thickness of 15 μm. Then a 70 nm-thick Ti/Au layer was sputtered and photolithographically patterned using wet etching according to an electrode design kindly provided by Multi Channel Systems. A 50 nm thick SiN layer was then deposited by plasma enhanced chemical vapor deposition (PE-CVD) and holes were dry etched to expose the Ti/Au layer only at the measuring dots, while leaving the rest electrically passivated. The PI with micro-electrode arrays (MEAs) was then locally delaminated from the glass carrier at the contact pad area. The resulting flexible contact pad area was flipped over the long edge of the glass/PI/MEA substrate and integrated with a 96-well microtiter plate modified with adhesive (ProPlate®).

2.2. Microfluidics fabrication

Microfluidic distribution channels were fabricated using a photopatternable resist of 45 μm thickness provided by Tokyo Ohka Kogyo (TOK) CO., LTD, that is either spin coated (TMMR® S2000) or laminated (TMMF® S2000) on a glass carrier (1.1 mm, EAGLE XG®). UV-photolithography exposure and photoresist development were then employed to structure the microfluidic channel at each resist layer, if needed. The process can be repeated multiple times to obtain even more complex fluidic structures. The microfluidic layers can then be lasered to isolate single devices which can also be delaminated from the glass carrier, resulting in a free-standing microfluidic device that is only 135 μm thick.

2.3. Biocompatibility test of microfluidics

The ISO 10993-5:2009 protocol was used. Upon sterilization with ethanol 70% (30 min) and washing with PBS (phosphate-buffered saline) (thrice), L929-fibroblast cells were seeded on the material photoresist and maintained in Eagle's minimum essential medium, EMEM (ATCC® 30–2003™), culture medium supplemented with 10% FBS (Sigma F7524), 1% penicillin/streptomycin (100 μg/ml, Lonza DE 17-602E) and 4 mM glutamine (Lonza17-605c). A monolayer of cells was grown, demonstrating that the photoresist employed does not influence the cell culture. Following the ISO protocol, adhesion, direct and indirect assays were performed based on the activity of living cells *via* mitochondrial dehydrogenases with 3-[4,5-dimethylthiazole-2yl]-2,5-diphenyltetrazolium bromide (MTT, Sigma TOX1-1KT).

Cell viability was assessed by fluorescent labelling with calcein AM (1 μg/ml, Sigma 17,783) for alive cells (green) and propidium iodide (4 μg/ml, Sigma P4170) for dead cells (red) with keratinocyte cell line (HaCaT).

3. Results and discussion

3.1. Micro electrode arrays and biocompatibility

FPD technology is the industrial standard for display manufacturing, where intricated matrixes of electrical interconnection are employed to select thin-film-transistors (TFTs) that drive each pixel of a display [14]. State-of-the-art FPD plants employ up to Gen 10.5 mother glass substrates (284 × 337 cm^2). Potentially this would allow to fabricate almost ~9000 SMWPs (12.7 × 8.5 cm^2) on the same substrate. More realistically, existing Gen 4.5 fabs could be partially converted to OoC and biomedical device production, thereby enabling the commercialization of devices in this domain. Therefore, FPD would be an ideal candidate for producing MEAs that are relevant, for example, in electrical cell-substrate impedance sensing (ECIS) to evaluate cell growth, morphology and function, or to spatio-temporally map the changes in extracellular field potential [15]. Details about the MEA fabrication are given in the Experimental Section. To demonstrate the large area scalability, 8 full SMWP MEA designs were fabricated within our Gen 1 (32 × 35 cm^2) FPD pilot-line, see Fig. 1a. We fabricated MEAs on PI which can be (partially) de-bonded, resulting in a thin flexible, semi-transparent foil that was integrated into a standard 96-well plate, as shown in Figs. 1 b) and c). This integration allows *in vitro* electrophysiology in microtiter plates, the *de facto* standard format for experiments in microbiological and pharmaceutical laboratories. Additionally, our semi-transparent MEA substrate enables optical transmission measurements or inspections from the bottom side of the well-plate.

Since photoresists and etching baths are involved in the lithography steps, the biocompatibility of the resulting microelectronics module, was tested to ensure the suitability of the fabrication process towards cell-culturing. To assess the biocompatibility, tests using human embryonal kidney cell line, HEK293 cells, were performed. Figs. 1 d) and e) show one of the MEA units before and 4–5 h after cell seeding, using a 50 μl cell suspension. No signs of cytotoxicity were observed after 4–5 h and the cells were attached to the bottom of the plate. After 3 days the cells expanded reaching 60%, 70%, 80% and 90–95% confluency for 20 μl, 25 μl, 30 μl and 50 μl cell suspension, respectively. It was therefore concluded that the MEAs on foil are well suited for HEK293 cell-culturing and thus confirmed the biocompatibility with the investigated cell line. In addition, fluorescence measurements were also performed, using green fluorescent protein (GFP) [16]. Figs. 1 f) and g) show the autofluorescence image taken before seeding cells with 70% fluorescence intensity, and 1 day post transfection with 30 μl cell suspension and same fluorescence intensity. From these tests it could be derived that cells with and without GFP can attach and grow in the wells. The GFP fluorescence signal could be clearly observed with an intensity comparable to stained cells in a standard 3.5 cm Petri dish

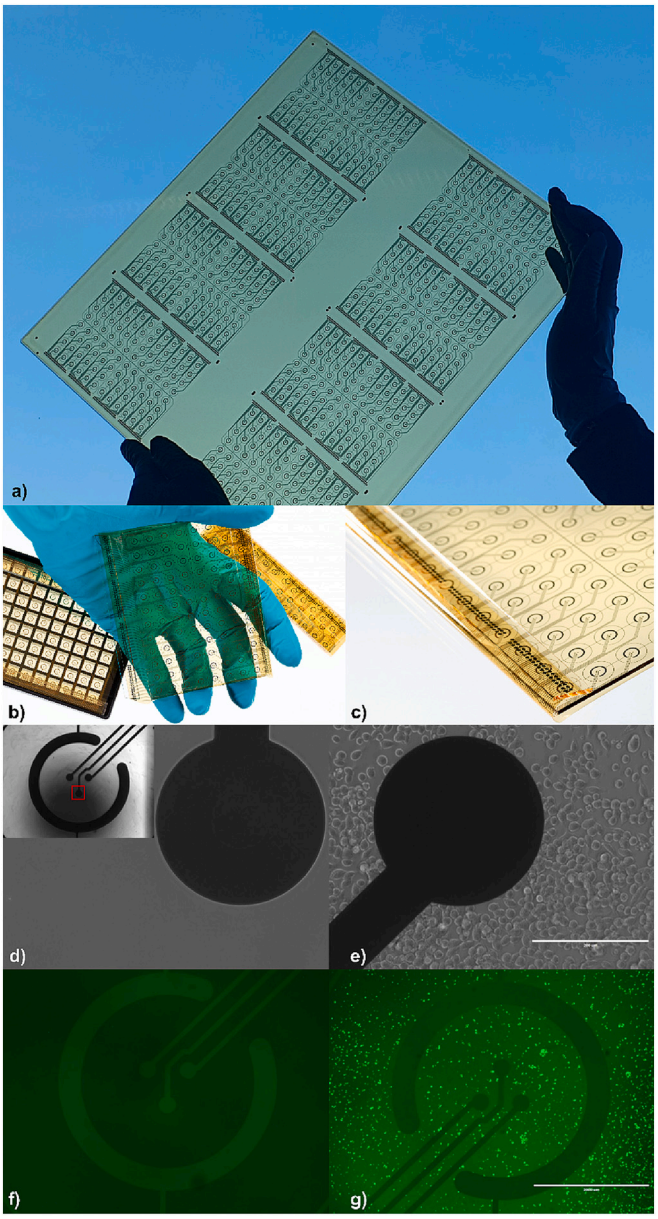

Fig. 1. a) 32 × 35 cm^2 glass plate with 8 × 96 well-plate format MEAs b) MEAs on polyimide foils glued onto a 96 well-plate, partially de-bonded from a glass carrier and fully de-bonded and rolled-out, c) close-up of the contact pads that are flipped over the long edge of the MEAs substrate. Microscope image of one electrode before d) and after e) cell seeding; the scale bar is 200 µm. Fluorescence images without f) and with cells g); the scale bar is 2000 µm.

before splitting, thus demonstrating the aptness of FPD fabrication technology for cell culturing and fluorescence measurements.

3.2. Microfluidics and biocompatibility

Microfluidics are essential components for biological devices as they allow for perfusing cell cultures with nutrients, removing metabolites and automating the delivery of drugs, for example. Microfluidic distribution channels (Fig. 2) were fabricated using a photo-patternable dry resist (see Experimental Section for details) and lamination onto a glass carrier. The microchannels were fabricated using a three-layer lamination process. Level 1, corresponding to flow-in and connection to level 2; level 2, to fluidic channel and connections to levels 1 and 3; level 3 corresponding to flow-out. Debonding from the glass carrier, resulted in

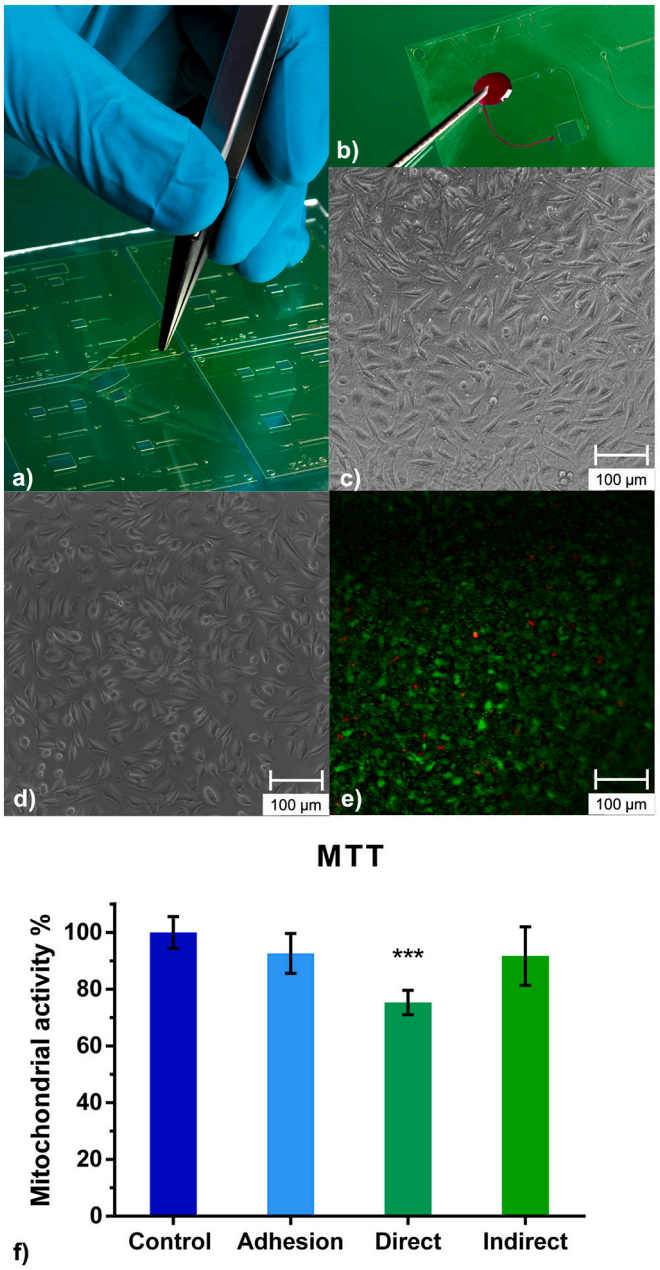

Fig. 2. Ultra-thin microfluidic distribution layer on a) glass carrier and b) after debonding. L929 cells on photoresist surface of c) direct and d) indirect assay. e) Fluorescence images of alive cells (green)/dead cells (red) overlayed. f) Mitochondrial activity in percentage for control sample, adhesion test, direct and indirect assay. *** $p < 0.001$ (Unpaired *t*-test). (For interpretation of the references to colour in this figure legend, the reader is referred to the web version of this article.)

a 135 µm thick free-standing microfluidic device, see Fig. 2a. The functionality of the microfluidic channels was tested by loading Rhodamine B dye in water with a syringe at the entrance of the channel as shown in Fig. 2b.

The biocompatibility of the materials employed to realize the device was also tested. To this end the ISO 10993-5:2009 protocol was used. The photoresist provides a surface on which cells are attached after 4 h of seeding, similarly (92%) to a positive control sample, see Fig. 2f. Direct assay (Fig. 2f) indicates that the cells in direct contact with the photoresist after 24 h have over 70% of the initial mitochondrial activity, thus the material can be considered biocompatible. Finally, the

photoresist employed for the microfluidic distribution layer did not liberate any toxic compounds since 91% of the mitochondrial activity could still be observed in the cells with conditioned medium in the indirect assay (Fig. 2d and f), implying biocompatibility with cell culturing.

Moreover, cell viability was assessed by fluorescent labelling. After 96 h of cell culturing on the photoresist >90% cell viability was observed (Fig. 2e).

3.3. Monolithic integration of microelectronics and microfluidics

The viability of FPD technology to realize OoC-devices was further supported by the monolithic integration, *i.e.* sequential processing of device layers on top of each other, of microelectronic and microfluidic *modules*. In a first example we integrated electrostatic valves with microfluidics. A second example shows the integration of MEAs with microfluidics. Fig. 3a shows a 15 × 15 cm^2 plate with microfluidic valves based on the concepts proposed by Micronit and IBM [17,18]. The basic underlying principle is that changes in geometry of a microfluidic channel can lead to pinning of the liquid, *i.e.* the flow becomes zero and the valve is effectively closed; upon applying a voltage pulse the flow can be restored, *i.e.* the valve is opened. Figs. 3c and d show one valve in the closed and open state, respectively, after applying a voltage pulse.

Fig. 4e shows an exploded schematic view of the monolithic integration of MEAs and microfluidics, together with microscopic images of different time frames of the device under microfluidic testing conditions. Here, the microfluidic layer was inspired by the phase-guide concept developed by Vulto et al. and commercialized by Mimetas [19,20]. Such device is made of three photoresist layers. In the bottom layer, the three microfluidic channels are separated, whereas in the second photoresist layer they merge into a single wider channel, as shown in Fig. 4e. In this way, 'restrictions' of 45 μm in height are created between the three channels and that forces fluid 1 (water with Rhodamine B) to remain pinned in the central fluidic channel without flooding the two side channels, see Figs. 4a and b. Upon pinning and settling of fluid 1, fluid 2 is introduced in the bottom left and right wells. For demonstration purposes a fluorinated liquid was used to ensure non-mixing between fluid 1 and fluid 2. The menisci of fluid 2 filling-up the side channels are highlighted with white arrows at two different frames, Fig. 4c and d, demonstrating the working principle of this fluidic design.

ECIS electrodes, aligned to the central microfluidic channel, are present in each well so that cells can be potentially cultured and measured in the middle channel, while the two side channels can be employed for providing nutrients and eventually purging metabolites. Overall, the device shown in Fig. 4 is an excellent example that shows the versatility and potential of FPD technology with respect to integrating microfluidics and microelectronics.

4. Conclusions

We have demonstrated the capabilities and potential of FPD technology for the fabrication of microelectronic and microfluidic modules

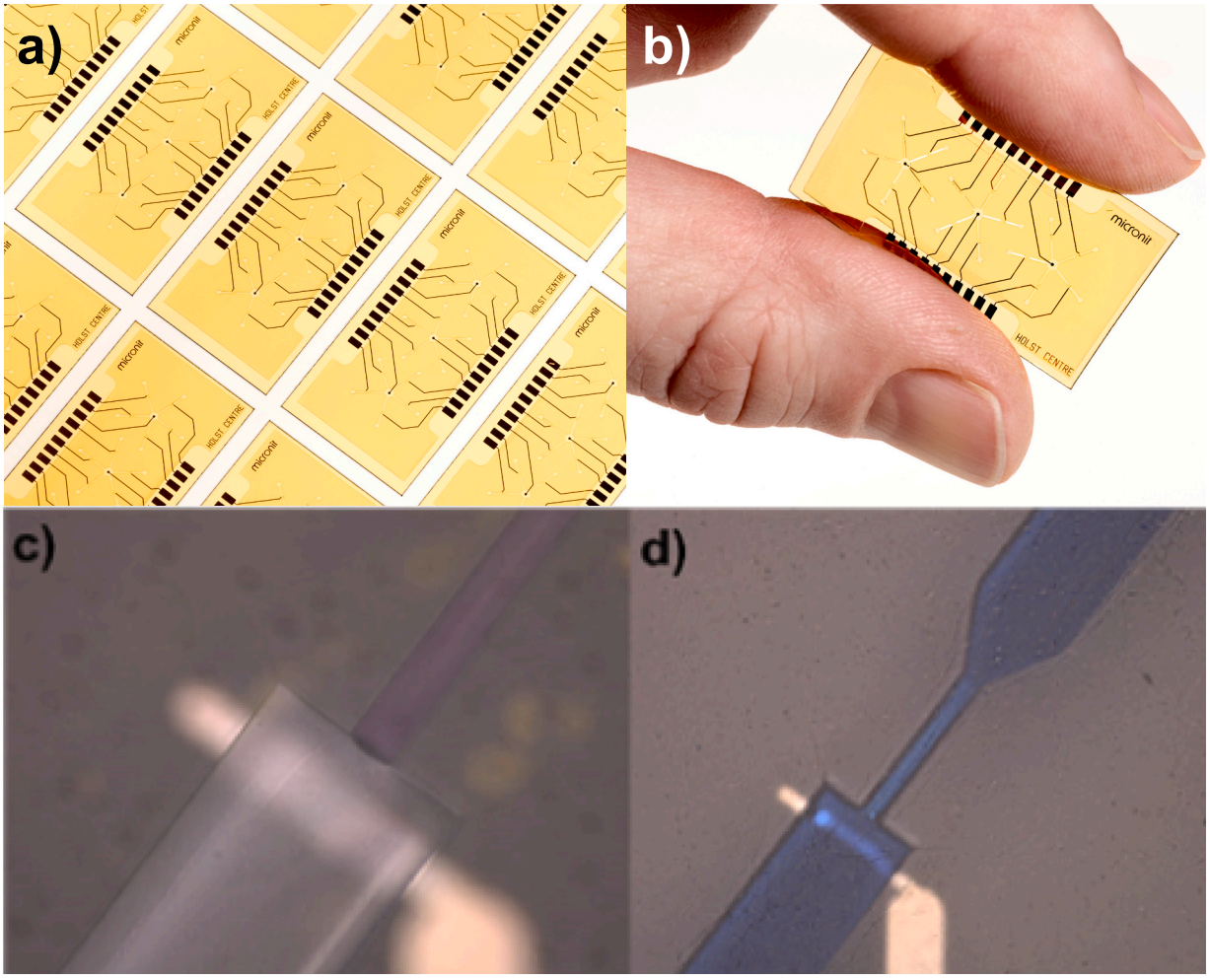

Fig. 3. Monolithic integration of microelectronics and microfluidics. a) electrostatic valves realized on polyimide on a glass carrier 15 × 15 cm^2. b) close-up picture of electrostatic valves devices. Microscope image of one valve in c) closed and d) open state.

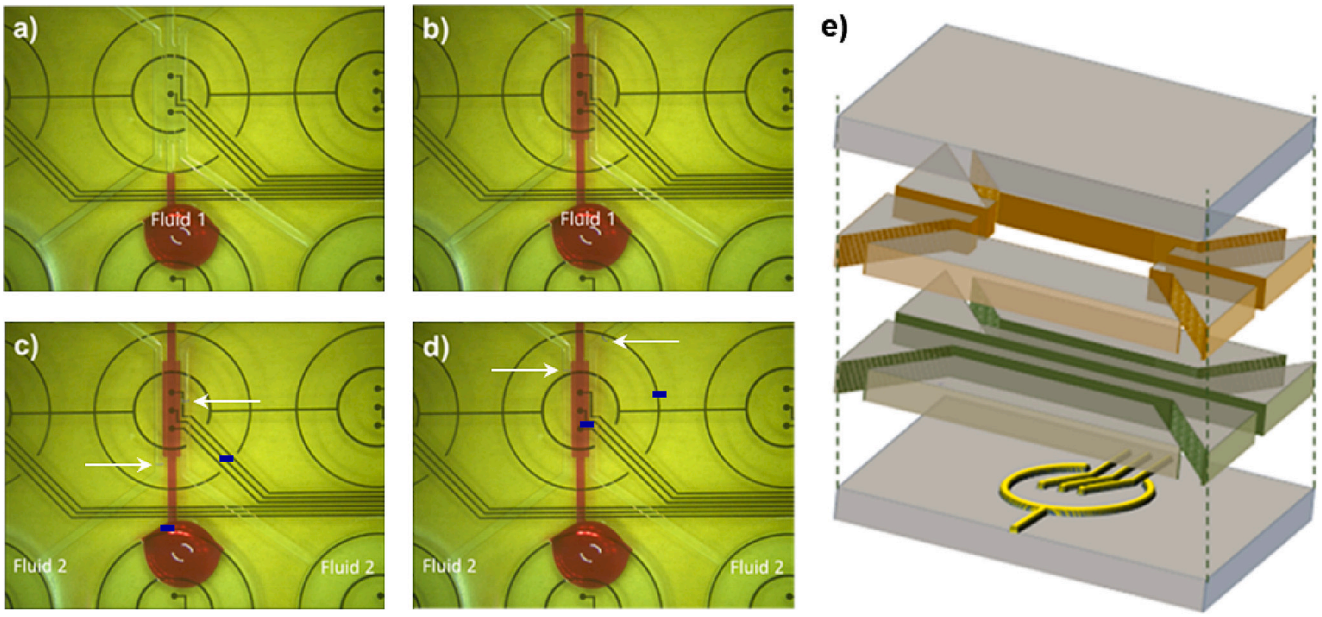

Fig. 4. Integrated MEA-based ECIS sensor and microfluidic channels for cell culturing and side channels for perfusion of nutrients. a)-d) different stages of filling microfluidic channels. e) schematic build-up of microfluidic channels with integrated ECIS electrodes.

and its integration in standardized smart multi-well plates. Micro electrode arrays and electrostatic valves have been monolithically integrated with dry-film resist based microfluidics to be used in biomedical applications like organ-on-chip and lab-on-chip.

Furthermore, we confirmed the biocompatibility of these modules and hence of the FPD technology using HEK293 and L929-fibroblast cells.

A general benefit of FPD technology for OoC applications is that the same production line can be used for both microfluidics and electronics, as we have demonstrated in this work. Furthermore, even more complex structures, electronics and sensor functionalities can be enabled by FPD technology which may not be straightforward to implement with more commonly used OoC rapid prototyping methods.

We believe that the approach presented in this work will increase the technology readiness level and enable cost-effective and robust fabrication that in turn will facilitate widespread adoption of standardized OoC and related biomedical devices.

Credit author statement

Alfredo Mameli, Hylke B. Akkerman, Sandra González-Lana, Héctor Castro-Abril, Kim Le Cann, Angelika Lampert were responsible for conceptualization, formal analysis, investigation and methodology. Alfredo Mameli and Albert van Breemen were responsible for writing the original draft. Alfredo Mameli, Gerwin, H. Gelinck, Auke Jisk Kronemeijer and Albert van Breemen were responsible for review & editing. All authors discussed and revised the final manuscript. Albert van Breemen supervised the project.

Declaration of Competing Interest

The authors declare that they have no known competing financial interests or personal relationships that could have appeared to influence the work reported in this paper.

Data availability

Data will be made available on request.

Acknowledgements

We gratefully acknowledge the collaboration with NMI TT, Multi-Channel Systems, Micronit, BEOnChip and AG Lampert Uniklinik RWTH Aachen University, providing valuable direction for entering the OoC application domain. Massimo Mastrangeli is acknowledged for fruitful discussions and critical comments. Part of this work is funded by the ECSEL JU Moore 4 Medical project, receiving funding under grant agreement H2020 ECSEL 2019 IA 876190.

References

[1] M. Mastrangeli, J. van den Eijnden-van Raaij, Stem Cell Reports 16 (2021) 2037.
[2] A.E. Danku, E.-H. Dulf, C. Braicu, A. Jurj, I. Berindan-Neagoe, Front. Bioeng. Biotechnol. 10 (2022) 1.
[3] K. Ronaldson-Bouchard, G. Vunjak-Novakovic, Cell Stem Cell 22 (2018) 310.
[4] Q. Ramadan, M. Zourob, Biomicrofluidics 14 (2020) 1.
[5] B.P. Johnson, R.A. Vitek, M.M. Morgan, D.M. Fink, T.G. Beames, P.G. Geiger, D. J. Beebe, R.J. Lipinski, Front. Cell, Dev. Biol. 9 (2021) 1.
[6] M. Mastrangeli, S. Millet, C. Mummery, P. Loskill, D. Braeken, W. Eberle, M. Cipriano, L. Fernandez, M. Graef, X. Gidrol, N. Picollet-D'Hahan, B. van Meer, I. Ochoa, M. Schutte, J. van den Eijnden-Van Raaij, ALTEX 36 (2019) 481.
[7] M. Piergiovanni, S.B. Leite, R. Corvi, M. Whelan, Lab Chip 21 (2021) 2857.
[8] M. Radisic, P. Loskill, A.C.S. Biomater, Sci. Eng. 7 (2021) 2861.
[9] H. Cong, N. Zhang, Biomicrofluidics (2022) 16, https://doi.org/10.1063/5.0079045.
[10] H. Azizgolshani, J.R. Coppeta, E.M. Vedula, E.E. Marr, B.P. Cain, R.J. Luu, M. P. Lech, S.H. Kann, T.J. Mulhern, V. Tandon, K. Tan, N.J. Haroutunian, P. Keegan, M. Rogers, A.L. Gard, K.B. Baldwin, J.C. de Souza, B.C. Hoefler, S.S. Bale, L. B. Kratchman, A. Zorn, A. Patterson, E.S. Kim, T.A. Petrie, E.L. Wiellette, C. Williams, B.C. Isenberg, J.L. Charest, Lab Chip 21 (2021) 1454.
[11] J.F. Wager, Inf. Disp. (1975) (36) (2020) 9.
[12] J. Smith, E. Bawolek, Y.K. Lee, B. O'Brien, M. Marrs, E. Howard, M. Strnad, J. Blain Christen, M. Goryll, Electron. Lett. 51 (2015) 1312.
[13] H. Akkerman, B. Peeters, A. van Breemen, S. Shanmugam, L.U. Lopez, D. Tordera, E. Delvitto, G. Simone, R. van de Ketterij, A.J. Kronemeijer, E. Meulenkamp, G. Gelinck, Dig. Tech. Pap. - SID Int. Symp. 52, 2021, p. 41.
[14] D.S. Ginley, H. Hosono, D.C. Paine, Handbook of Transparent Conductors, 2011.
[15] S. Fuchs, S. Johansson, A. Tjell, G. Werr, T. Mayr, M. Tenje, A.C.S. Biomater, Sci. Eng. 7 (2021) 2926.
[16] M. Zimmer, Chem. Rev. 102 (2002) 759.
[17] A. Tsopela, S. Meucci, S. Rocchiccioli, G. Pelosi, M. Brivio (2018) 390.
[18] Y. Arango, Y. Temiz, O. Gökçe, E. Delamarche, Appl. Phys. Lett. 112 (2018), https://doi.org/10.1063/1.5019469.
[19] M. Jang, P. Neuzil, T. Volk, A. Manz, A. Kleber, Biomicrofluidics 9 (2015) 1.
[20] P. Vulto, S. Podszun, P. Meyer, C. Hermann, A. Manz, G.A. Urban, Lab Chip 11 (2011) 1596.